Tailored Ring-Opening Metathesis Polymerization Derived Monolithic Media Prepared from Cyclooctene-Based Monomers and Cross-Linkers

Rajendar Bandari,[†] Andrea Prager-Duschke,[†] Christa Kühnel,[†] Ulrich Decker,[†] Bettina Schlemmer,[†] and Michael R. Buchmeiser*[,†,‡]

Leibniz Institut für Oberflächenmodifizierung e.V. (IOM), Permoserstrasse 15, D-04318 Leipzig, Germany, and Institut für Technische Chemie, Universität Leipzig, Linnéstrasse 3, D-04103 Leipzig, Germany

Received May 3, 2006; Revised Manuscript Received June 1, 2006

ABSTRACT: The synthesis of ring-opening metathesis polymerization (ROMP) derived monolithic media prepared from *cis*-cyclooctene (COE) as monomer, tris(cyclooct-4-ene-1-yloxy)methylsilane (CL) as cross-linker, toluene as microporogen, and 2-propanol as macroporogen is described. Monolithic supports with varying composition in terms of COE, CL, microporogen, and macroporogen were prepared using $RuCl_2(Py)_2$(1,3-Mes_2-imidazolin-2-ylidene)(CHC_6H_5) (Mes = 2,4,5-trimethylphenyl, Py = pyridine) and pyridine as modulator and characterized via inverse size exclusion chromatography (ISEC) and electron microscopy. Monoliths 3 × 100 mm in size were used for the separation of a mixture of five proteins, i.e., ribonuclease A, lysozyme, insulin, cytochrome *c*, and myoglobin. Semipreparative separation of these compounds was achieved within less than 150 s by applying gradient elution. Peak half-widths ($\omega_{0.5}$) were <6 s, and resolution (R_s) was >1.2 throughout. Functionalization of the novel support was accomplished in situ and exemplified by grafting various amounts of 7-oxanorborn-5-ene-2,3-dicarboxylic anhydride on the monolithic structure. By this approach, carboxylic acid loadings up to 86 μmol/g, corresponding to 0.71 wt %, were realized.

Introduction

Monolithic separation media evolved as a successful "joint venture" between material and separation science. Generally speaking, the term "monolith" applies to any single-body structure containing interconnected repeating cells or channels. Here, the term "monolith" or "rigid rod" comprises cross-linked, organic materials which are characterized by a defined porosity and which support interactions/reactions between this solid and the surrounding liquid phase. Based on theoretical reflections, the general idea is to produce a support with a high degree of continuity that meets the requirements for fast, yet highly efficient separations.[1,2] Besides advantages such as lower back-pressure and enhanced mass transfer,[3,4] the ease of fabrication as well as the many possibilities in structural alteration needs to be mentioned. The first experiments into this direction were carried out in the 1960s and 1970s,[5,6] yet it took some 20 years to adapt this new technology for the present purposes. On their way of evolution, these supports, usually referred to as monolithic supports, continuous beds, or rigid rods,[6] were successfully used in liquid chromatography including microseparation techniques,[7−10] chip,[11] and capillary electrochromatography as well as solid-phase extraction (SPE).[12] In these separation techniques, the focus was on both medium to high molecular mass biopolymers[13] and low molecular mass analytes.[14−17] There exist excellent reviews that provide a profound overview over this area of research.[18−22] In contrast to free radical polymerization-based syntheses, our group confirmed the general applicability of a transition-metal-based polymerization technique, i.e., ring-opening metathesis polymerization (ROMP), to the synthesis of high-performance monolithic separation media and described the use of these supports in separation science and heterogeneous catalysis.[23−36] So far, the ROMP-based synthetic protocol entailed the use of norborn-2-ene (NBE) as monomer and NBE-derived cross-linkers, e.g., tris(norborn-5-ene-2-ylmethyloxy)methylsilane or 1,4,4a,5,8,-8a-hexahydro-1,4,5,8-*exo*,*endo*-dimethanonaphthalene (DMN-H6). These compounds are readily polymerized using Grubbs' first-generation catalyst, $RuCl_2(PCy_3)_2(CHC_6H_5)$, to form the desired monolithic structure, which are in principle stable over the entire pH range since they solely consist of hydrocarbons. However, NBE-derived monomers result in polymer structures composed of *tertiary* allylic carbons (Figure 1). Despite the high mechanical and thermal stability of these structures,[25] which is by far sufficient for short- and medium-term analytical applications as well as applications in heterogeneous catalysis,[37] tertiary allylic carbons located at the surface of a monolithic structure tend to be oxidized, resulting in reduced long-term stabilities of monolithic columns. Thus, the typical long-term stability of NBE-based, ROMP-derived columns is limited to less than 1000 injections.

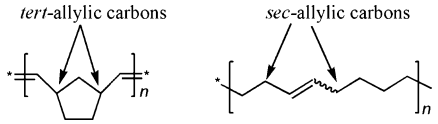

Figure 1. Polymer structures derived from NBE (left) and COE (right).

We therefore tried to solve this problem by introducing a novel monomer/cross-linker system to the synthesis of monolithic structures. For these purposes, we developed a polymerization system based on *cis*-cyclooctene (COE) and tris(cyclooct-4-en-1-yloxy)methylsilane (CL). Our efforts were guided by the idea that the polymer backbone of poly(cyclooctene)-derived materials consists of *secondary* allylic carbons and therefore presents an attractive alternative to NBE-based systems, though

* Corresponding author: e-mail michael.buchmeiser@iom-leipzig.de; tel ++49 (0) 341 235 2229; fax ++49 (0) 341 235 2584.
† Leibniz Institut für Oberflächenmodifizierung.
‡ Universität Leipzig.

10.1021/ma0609883 CCC: $33.50
Published on Web 07/07/2006

Scheme 1. Synthesis of Cross-Linker (CL)

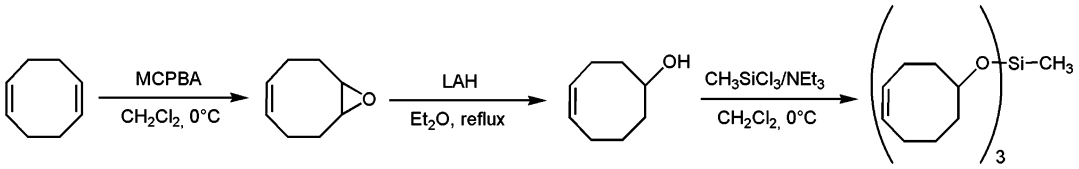

these compounds possess significantly reduced ring strain, thus requiring more active initiators. This and the use of novel monomers made the comprehensive redesign of monolith synthesis inevitable. Not unexpectedly, the resulting COE-based monolithic structures possessed significant differences compared to the parent NBE-based systems. Our results are summarized in the following.

Results and Discussion

Synthesis of the Cyclooctene-Based Cross-Linker (CL) and the Initiator. Following published protocols,[38] cycloocta-1,5-diene was reacted with *m*-chloroperbenzoic acid (MCPBA) to yield cycloocta-1,5-diene 1-oxide, which was then reduced with lithium aluminum hydride (LAH) to yield a mixture of enantiomeric 1-hydroxy-cyclooct-5-ene. The enantiomeric alcohols were used for the synthesis of the cross-linker tris(cyclooct-4-en-1-yloxy)methylsilane (CL) by reaction with methyltrichlorosilane (Scheme 1), yielding the target compound as an enantiomeric mixture of diastereomers.

$RuCl_2$(1,3-Mes_2-imidazolin-2-ylidene)(CHC_6H_5)($Py)_2$ (Mes = 2,4,6-trimethylphenyl, Py = pyridine) was prepared according to a protocol published by Grubbs et al.[39] via reaction of $RuCl_2$-(PCy_3)(1,3-Mes_2-imidazolin-2-ylidene)(CHC_6H_5) with excess pyridine in virtually quantitative yield. As is the case with the corresponding 2-Br-pyridine adduct, yet in contrast to complexes based on 1,3-dimesityltetrahydropyrimidin-2-ylidenes,[40] a complex containing two pyridine moieties instead of one phosphine group is obtained.

Choice of Polymerization System. The change from a pure NBE-based polymerization system, as realized by the use of NBE as a monomer and tris(norborn-5-ene-2-ylmethyloxy)-methylsilane or 1,4,4a,5,8,8a-hexahydro-1,4,5,8-*exo*,*endo*-dimethanonaphthalene (DMN-H6) as cross-linkers, to a pure *cis*-cyclooctene-based polymerization system requires significant changes in the structure of the initiator. As a consequence of the reduced ring strain in cyclooctenes, the reactivity of the initiator needs to be enhanced. In due consequence, the first-generation Grubbs' catalyst, $RuCl_2(PCy_3)_2(CHC_6H_5)$, was replaced by a fast initiating derivative of the second-generation Grubbs' catalyst, i.e., by $RuCl_2(Py)_2$(1,3-Mes_2-imidazolin-2-ylidene)(CHC_6H_5).[39] Irrespective of the nature of N-heterocyclic carbenes used for catalyst synthesis, such pyridine[39,40] or 2-Br-pyridine[41] adducts turned out to be fast-initiating initiators for ROMP, displaying high initiation efficiencies. To make reactivity feasible to the handling of the polymerization mixtures, i.e., to slow down kinetics, pyridine was added. Kinetic measurements on the polymerization of COE in the presence of different amounts of pyridine (0.8, 1.5, 3.0, 7.8, and 10.2 mol equiv with respect to initiator) were carried out in CH_2Cl_2 in order to determine the optimum polymerization conditions for monolith manufacture (Figure 2).

The values for $k_{p(obs)}$ determined there from were 0.11 min^{-1} (10.2 mol equiv of Py), 0.14 min^{-1} (7.8 mol equiv of Py), 0.27 min^{-1} (3.0 mol equiv of Py), 0.39 min^{-1} (1.5 mol equiv of Py), and 0.56 min^{-1} (0.8 mol equiv of Py). Assuming that similar to $RuCl_2(PCy_3)$(1,3-dimesitylimidazolin-2-ylidene)(=CHPh)[42] the dissociation of one pyridine molecule is necessary to provide the necessary free coordination site, the following equation[42] applies:

$$\frac{1}{k_{obs}} = \frac{k_{-1}[Py]}{k_1 k_2[COE]} + \frac{1}{k_1}$$

From the graph $1/k_{obs}$ vs [Py][COE] ($R^2 = 0.998$, Figure 3), a value of $1/k_1 = 1.27$ and $k_1 = 0.79$ min^{-1} can be determined. From $k_{-1}/k_1k_2 = 5.2 \times 10^5$ follows $k_{-1}/k_2 = 4 \times 10^5$. Two important conclusions can be drawn from these data. First, reaction appears to be first order in pyridine, and second, according to the value for k_{-1}/k_2, recoordination of pyridine with respect to addition of the alkene is much faster in the present system than observed for most PCy_3-based initiators.[42]

On the basis of these measurements, an additional amount of 0.8 mol equiv of pyridine with respect to the initiator was chosen throughout, since it resulted in a polymerization system that guaranteed both sufficient time for the handling of the

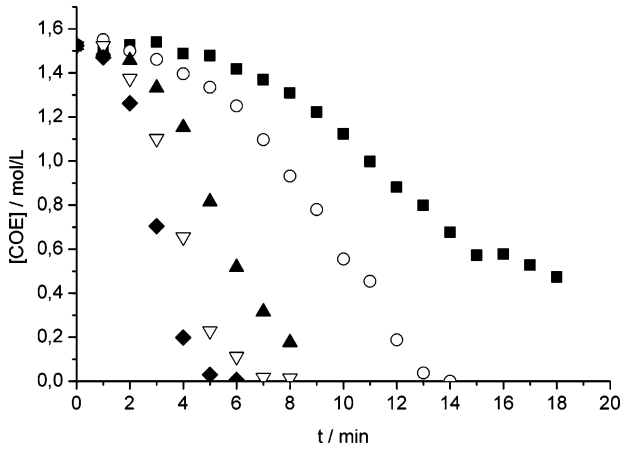

Figure 2. Polymerization kinetics of COE using $RuCl_2(Py)_2$(1,3-Mes_2-imidazolin-2-ylidene)(CHC_6H_5) as initiator and various amounts of pyridine: (■) 10.2 mol equiv of pyridine, (○) 7.8 mol equiv of pyridine, (▲) 3.0 mol equiv of pyridine, (▽) 1.5 mol equiv of pyridine, (◆) 0.8 mol equiv of pyridine.

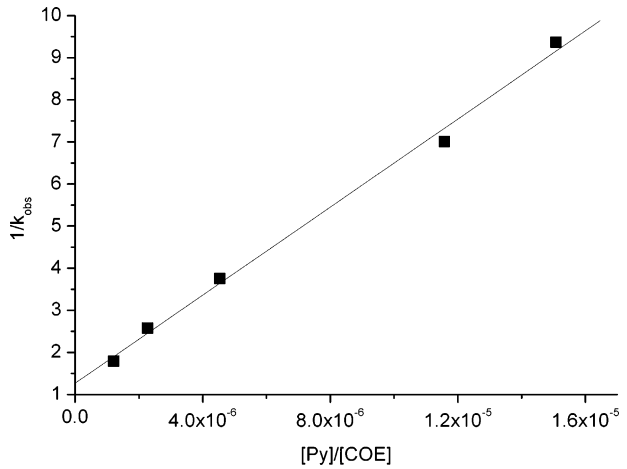

Figure 3. Graph $1/k_{obs}$ vs [Py][COE] ($R^2 = 0.998$) for different amounts of free pyridine added to the polymerization system.

Scheme 2. Synthesis of Monoliths

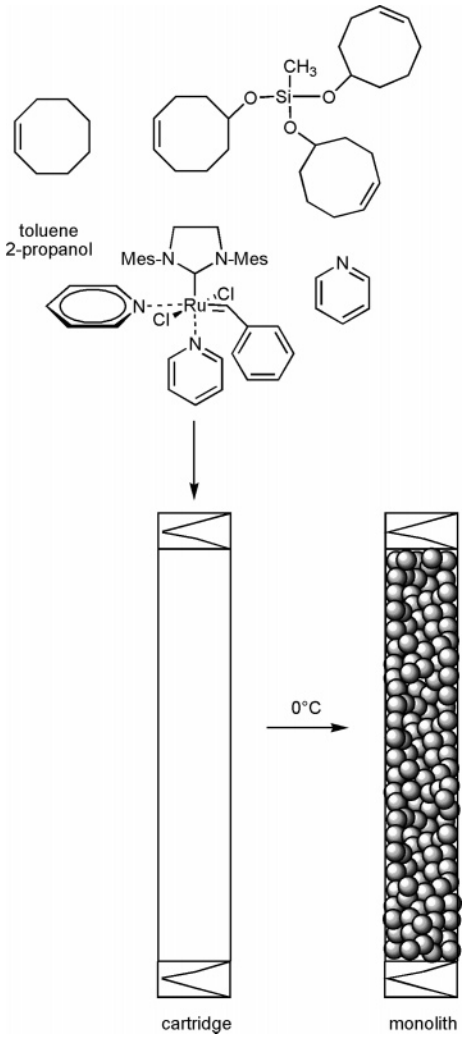

mixture, i.e., transfer into the column, and sufficient fast polymerization. Similar to previously reported NBE-based system, the final polymerization system consisted of various amounts of the monomer (COE), the cross-linker (CL), 2-propanol as a macroporogen, and toluene as microporogen. In addition to the amount of pyridine mentioned above (0.8 mol equiv with respect to initiator), an initiator loading of 0.2 wt % was chosen throughout. For monolith synthesis, COE and the CL were dissolved in 2-propanol. A second solution was prepared by dissolving the initiator and pyridine in toluene. Both solutions were chilled to 0 °C and mixed for 30 s, and the mixture was transferred into the column (see Experimental Section, Scheme 2).

Polymerization was allowed to proceed for 30 min at 0 °C, followed by 16 h at room temperature. The columns were then cleaned and placed inside a cartridge holder, and the monolith was cleaned by flushing with a solution of ethyl vinyl ether (20 wt %) in dimethyl sulfoxide.[36] This capping procedure ensured the complete removal of all Ru compounds as evidenced by ICP-OES measurements. Thus, the final Ru content in the monolithic rod was 33 ppm or less (i.e., below the limit of detection of the ICP-OES). After this procedure the monoliths were ready for use and characterization.

Characterization of the Microstructure of COE/CL-Based Rigid Rods. A description of the general construction of a monolith in terms of microstructure, backbone, and relevant abbreviations is given elsewhere.[23,24] In brief, monoliths consist of interconnected microstructure-forming microglobules, which are characterized by a certain mean particle diameter (d_p) and microporosity (ϵ_p). In addition, the monolith is characterized by an intermicroglobule void volume (ϵ_z), which is mainly responsible for the back pressure at a certain flow rate. Microporosity (ϵ_p) and intermicroglobule porosity (ϵ_z) add up to the total porosity (ϵ_t), which indicates the total porosity as a percentage of all types of pores within the monolith and from which the total pore volume (V_p), expressed in μL/g, may be calculated.[43] The pore size distribution is best calculated from inverse size exclusion chromatography (ISEC) data.[43,44] In addition, one may calculate the specific surface area (σ), expressed in m^2/g, therefrom.

As mentioned, the entire polymerization mixture consists of COE, CL, pyridine, toluene, and 2-propanol and is therefore quite complex and may additionally be influenced by temperature. Thus, the relative ratios of all components allow for broad variations in the microstructure of the monolithic material; however, the resulting structures of the monoliths in terms of d_p, ϵ_z, ϵ_p, V_p, and σ are not formed randomly. To check for the influence of all variables, i.e., components of the polymerization mixture (COE, CL, porogens, i.e., the two solvents) on microstructure formation, a series of variations were carried out. The tremendous influence of increased amounts of pyridine on the structure of the resulting monoliths became clear from comparing monoliths **2** and **2a**. Thus, changing the amount of free pyridine from 0.8 to 1.5 mol equiv resulted in an increase in particle diameter, a decrease in porosity (both ϵ_z and ϵ_p), and a decrease in specific surface area. Using a total monomer content (COE + CL) of 60%, the volume fraction of the interglobular void volume (ϵ_z) could be varied in the range 16−35% (Table 1). Higher total monomer contents led to impervious columns, i.e., to structures with insufficient amounts of interpenetrating pores, whereas lower monomer contents resulted in elastic, rubber-type monoliths. Monoliths prepared from pure CL did not show any meso- or macroporosity.

With the structural variations carried out, the volume fraction of the pore volume could be adjusted within the range 7−28%. These values resulted in total porosities (ϵ_t) within the range 43−57%. These figures demonstrate that packing density strongly correlates with the total monomer content, as is also visualized in Figure 4.

In addition, an increase in the COE content of the polymerization mixture can be correlated with an increase in ϵ_p, directly translating into an increase in specific surface area (σ). However, it should be noted that there is no linear correlation. A more detailed analysis of the monolith's structure is provided in Figures 5−7.

They show the relative abundance of pores in the 5−10.000 Å region. What becomes evident from these measurements is that a fairly even pore size distribution may only be accomplished by using COE + CL contents ≥50% as realized in the recipes for monoliths **4**, **8**, and **9**. Here microporosity is reduced at the expense of larger pores. The most homogeneous distribution was realized with monolith **4**. The most striking feature of COE-based systems is their structural difference from NBE-derived ones as is observed with monoliths prepared from COE/CL (monoliths **3** and **8**) and NBE/DMN-H6 (monoliths **10** and **11**). These two sets of monoliths differ significantly in that the COE-based structures exhibit significantly reduced values for ϵ_z, yet higher values for ϵ_p and V_p compared to their NBE-based counterparts. This is a very important finding, since it has ultimate impact on separation issues (vide infra).

Table 1. Composition (in wt %) and Structural Data of Monoliths 1−14

monolith	COE	CL	2-PrOH	toluene	initiator	ϵ_p (%)	ϵ_z (%)	ϵ_t (%)	d_p (μm)[e]	V_p (μL/g)	Φ_m (Å)	σ (m^2/g)
1	5	35	40	10	0.2	7	46	53	5.3	320	560	23
2	20	20	50	10	0.2	13	35	48	5.6	580	360	64
2a[f]	20	20	50	10	0.2	9	26	36	6.5	290	810	14
3	22.5	22.5	42.5	12.5	0.2	22	35	57	8.4	500	250	83
4	25	25	40	10	0.2	17	32	49	2.0	560	600	38
5	30	30	30	10	0.2	24	28	52	6.0	550	230	96
6	30	10	50	10	0.2	22	26	49	7.5	960	220	171
7	30	20	40	10	0.2	22	29	51	5.2	580	220	104
8	35	15	40	10	0.2	27	16	43	6.0	910	480	76
9	35	25	30	10	0.2	28	19	47	3.0	760	300	100
10	22.5 NBE	22.5 DMN-H6	42.5	12.5	0.4	10	56	66	4.0	310	760	16
11	35 NBE	15 DMN-H6	40	10	0.2	12	34	46	2.2	440	150	115
12[a,b]	20	20	50	10	0.2	15	42	47	n.d.	390	260	59
13[a,c]	22.5	22.5	42.5	12.2	0.2	20	32	52	n.d.	620	290	85
14[a,d]	25	25	40	10	0.2	15	26	41	n.d.	370	460	32

[a] Functionalized with 7-oxanorborn-5-ene-2,3-dicarboxylic anhydride. Capacities determined by titration. [b] 52 μmol of COOH/g. [c] 82 μmol of COOH/g. [d] 86 μmol of COOH/g. [e] Mean particle diameter ($n = 30$). [f] 1.5 mol equiv of pyridine.

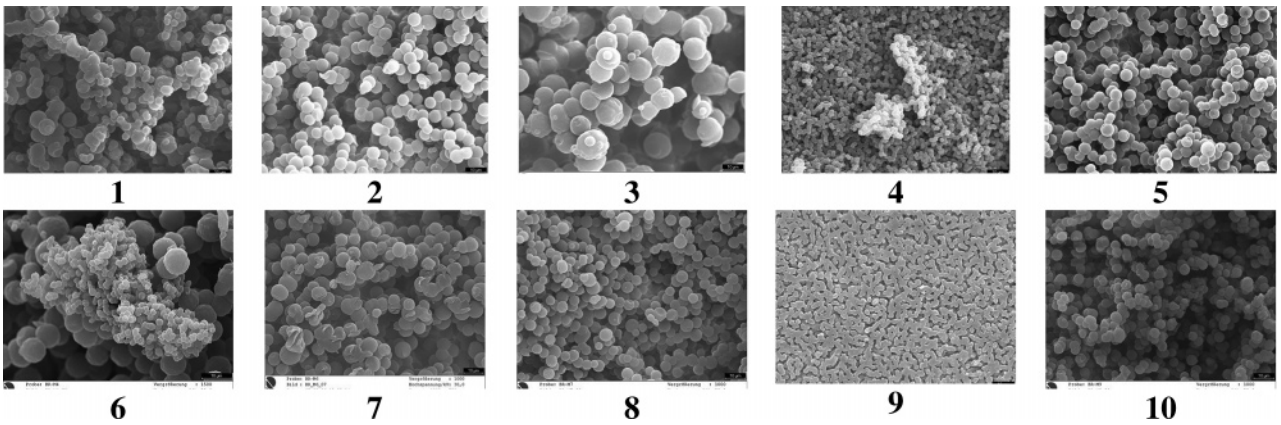

Figure 4. Structure of monoliths **1**−**10**.

Separation of Proteins. Separation of a mix of proteins, i.e., ribonuclease A, lysozyme, insulin, cytochrome *c*, and myoglobin, was carried out applying gradient elution. Figure 8 illustrates the fast separation of these compounds, which was accomplished in less than 150 s. Peak half-widths ($\omega_{0.5}$) were <6 s, and resolution (R_s) was >1.2 throughout.

For purposes of comparison, an NBE-based monolith of the same recipe, i.e., using the same amounts of monomer, cross-linker, and porogens, was synthesized and used for separation. When the identical gradient was applied, peak half-widths ($\omega_{0.5}$) were <7 s and resolution (R_s) was >1.1 throughout. Since lysozyme ($M_w = 14\,307$) and ribonuclease ($M_w = 13\,700$) are well separated ($R_s = 10.6$!), separation must be considered independent from molecular weight but is certainly a function of the *tertiary structure* of the corresponding analyte. The most striking difference in separation behavior of both COE- and NBE-based columns is observed in the retention times of the analytes as well as in R_s and the values for the mean peak half-width ($\omega_{0.5}$). These findings can be related to the structural data obtained via ISEC for both monoliths **8** (COE-based) and **11** (NBE-based). On the one hand, the NBE-derived column shows a more distinct pore size distribution with a local maximum for pore diameters between 40 and 80 Å. This translates into molecular weights of 2000−4000 g/mol (calculated for PS in CH_2Cl_2). On the other hand, the analytes used show higher molecular weights throughout ($M_w = 5733$−$17\,600$ g/mol), and the hydrodynamic volume of a protein with a certain molecular weight in water is expected to be higher than that of PS of the same molecular weight in CH_2Cl_2. Therefore, the enhanced analyte retention on NBE columns is currently attributed to interactions of *parts of* the analytes with surface structures inside the pores in the 40−80 Å region and not to size exclusion effects. Further experiments will be needed to fully address this point.

Functionalization of COE-Based Monoliths. As already demonstrated for ROMP-derived, NBE-based monoliths, functionalization may be accomplished conveniently taking advantage of the "living" character[45−50] of ruthenium-catalyzed polymerizations. Tentacle-like polymer chains attached to the surface are formed. To check whether this concept of in-situ functionalization could also be used for COE/CL-derived monoliths, we conducted functionalization using 7-oxanorborn-5-ene-2,3-dicarboxylic anhydride as a monomer. Grafting of this monomer in fact resulted in functionalized monoliths **12**−**14** with loadings of 52−86 μmol of COOH/g, corresponding to 0.43−0.71 wt % of monomer. As expected, pore sizes shifted to larger mean pore diameters at the expense of smaller pores (monolith **13** vs monolith **3**). With the exception of monolith **12**, this shift is also reflected by a (slight) reduction in the values for ϵ_p, ϵ_z, and V_p. Values for the specific surface area were basically retained.

Experimental Section

Methods and Materials. All manipulations were performed under an Ar atmosphere in an MBraun glovebox or by using Schlenk techniques. Narrow polystyrene (PS) standards with molecular masses (M_w) of 972, 2600, 4000, 6810, 17 200, 94 650, 803 000, 3 390 000, and 4 110 000 g/mol were purchased from Waters. In addition, narrow PS standards with molecular masses (M_w) of 4000, 30 000, 200 000, 400 000, and 900 000 g/mol were purchased from Polymer Standards Service (PSS, Pittsburgh, PA). Chloroform (99.5%) was purchased from KMF Laborchemie

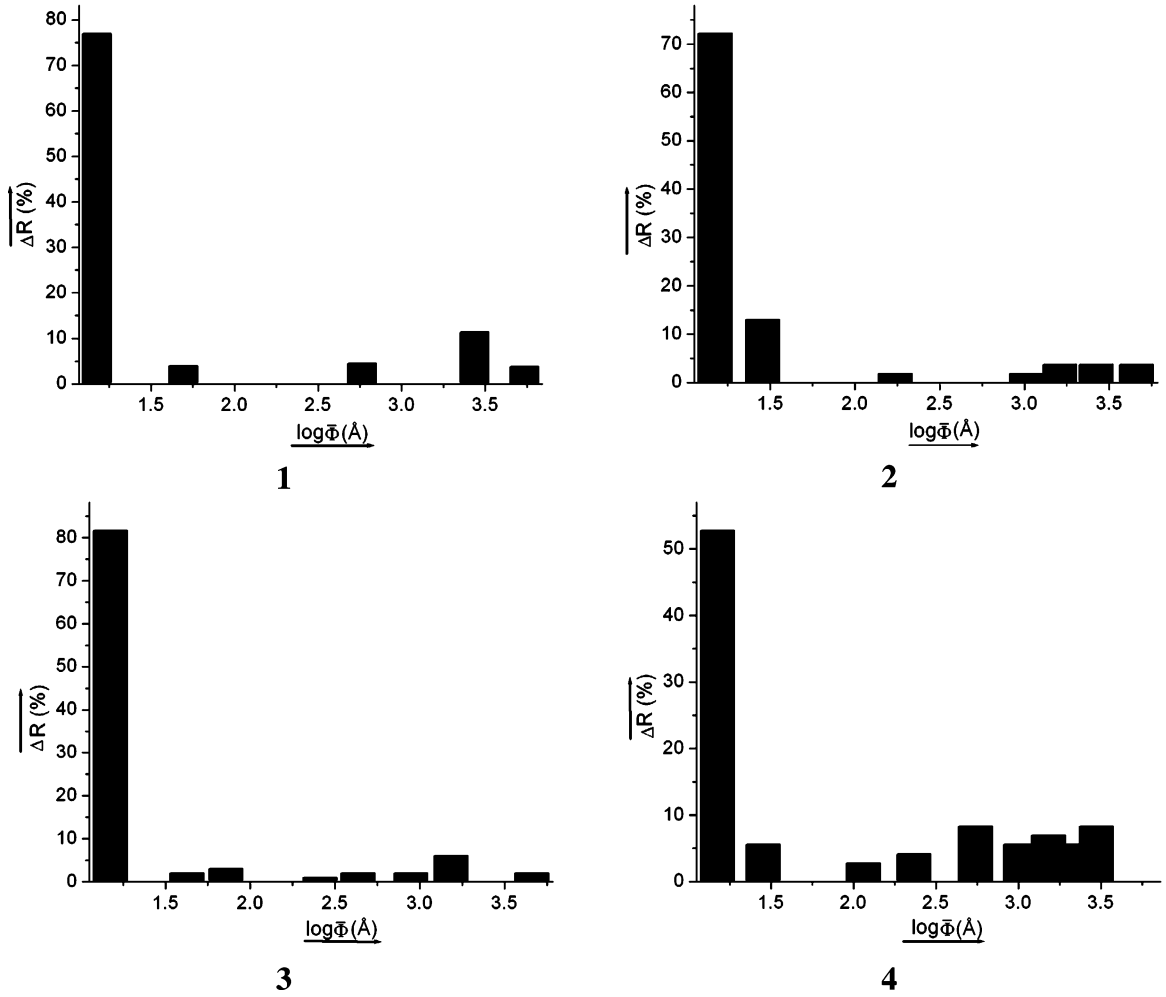

Figure 5. Log $\Phi_{average}$ (Å) vs ΔR (%) for monoliths **1**−**4**.

Handels GmbH (Germany), dried over CaH_2, and distilled prior to use. [$RuCl_2(PCy_3)(IMesH_2)(CHPh)$] ($IMesH_2$ = 1,3-bis(2,4,6-trimethylphenyl)imidazolin-2-ylidene), PCy_3 = tricyclohexylphosphine), *m*-chloroperbenzoic acid, $LiAlH_4$, 1,5-cyclooctadene, *cis*-cyclooctene, ethyl vinyl ether, and dimethyl sulfoxide were obtained from Aldrich Chemical Co. (Germany) and used as received. Acetonitrile, water (HPLC-grade), trifluoroacetic acid (99.5%), ribonuclease A (from bovine pancreas, M_w = 13 700 g/mol), lysozyme (from chicken egg white, M_w = 14 307 g/mol), insulin (from bovine pancreas, M_w = 5733 g/mol), cytochrome *c* (from bovine milk, M_w = 13 000 g/mol), myoglobin (from horse skeletal muscle, M_w = 17 600 g/mol), and the peptide separation buffer (PSB) were purchased from Sigma-Aldrich Co, Germany. 4-Cycloocten-1-ol was prepared according to the literature.[38] Triethylamine (Fluka, Switzerland) was dried over CaH_2 and distilled prior to use. Diethyl ether, toluene, and methylene chloride were dried by an MBraun SPS solvent drying system. NMR data were obtained at 250.13 MHz for proton and 62.90 MHz for carbon in the indicated solvent at 25 °C on a Bruker Spectrospin 250 and are listed in parts per million downfield from tetramethylsilane for proton and carbon. IR spectra were recorded on a Bruker Vector 22 using ATR technology. GC-MS investigations were carried out on a Shimadzu GCMS QP5050, using a SPB-5 fused silica column (30 m × 0.25 μm film thickness). The column He flow was set to 1.0 mL/min. For SEC and inverse (ISEC) measurements, an L-4500 UV detector (Merck) and an L-6200A HPLC pump (Merck) equipped with a manual sample injection system were used. A D-7000 HPLC system was used for data acquisition and processing. All standards were prepared by dissolving the peptides of interest in the peptide separation buffer (PSB) followed by further dilution with mobile phase and stored at −20 °C. HPLC measurements were carried by use of an SCL-10 AVP system controller, an LC-10AT HPLC pump, an SIL-10A autoinjector, an SPD-M10AVP diode array detector, a CTO-10AC column oven, and CLASS-VP503 software (all by Shimadzu). Eluents were degassed with He. High-resolution mass spectra (HRMS) were recorded via electron spray ionization (ESI) technique using a FT-ICR-MS Bruker Daltronics APEX II instrument. A CIROS System (Spectro A.I., Kleve) was used for ICP-OES measurements and an MLS 1200 mega for microwave experiments. Programming: 20−180 °C in 15 min, another 15 min at 180 °C, then to 20 °C within 1 h.

General Procedure for the Preparation of Monoliths. All monoliths for ISEC experiments were prepared as follows. Stainless steel columns (150 × 4.6 mm i.d.) were cleaned, rinsed, and sonicated in a 1:1 mixture of ethanol and acetone. Columns (3 × 100 mm) used for protein separation were treated as described earlier.[25] Columns were then dried for 2 h in vacuo and after that closed at one end with frits and end fittings and cooled to 0 °C. Separately, two different solutions (A, B) were prepared and cooled to 0 °C. Solution A consisted of *cis*-cyclooctene, tris(cyclooct-4-en-1-yloxy)methylsilane (CL), and 2-propanol, while solution B consisted of a solution of the initiator [$RuCl_2(Py)_2(IMesH_2)(CHPh)$] (0.2 wt %) and pyridine (0.018 wt %) in toluene. Both solutions were merged at 0 °C and mixed for ca. 30 s. The column was filled with the polymerization mixture, then sealed with Teflon caps, and kept at 0 °C for 30 min. After rod formation was finished, the column was closed, and each monolith was stored at room temperature for 16 h. To remove the initiator and excess of COE and CL, columns were provided with new frits and flushed with a mixture of 20 vol % ethyl vinyl ether in dimethyl sulfoxide for 8 h at a flow rate of 0.1 mL/min. Finally, they were flushed with chloroform for 4 h at a flow rate of 0.2 mL/min.

Functionalization of Monoliths. For functionalization, the same method as mentioned above was used. After the columns were kept

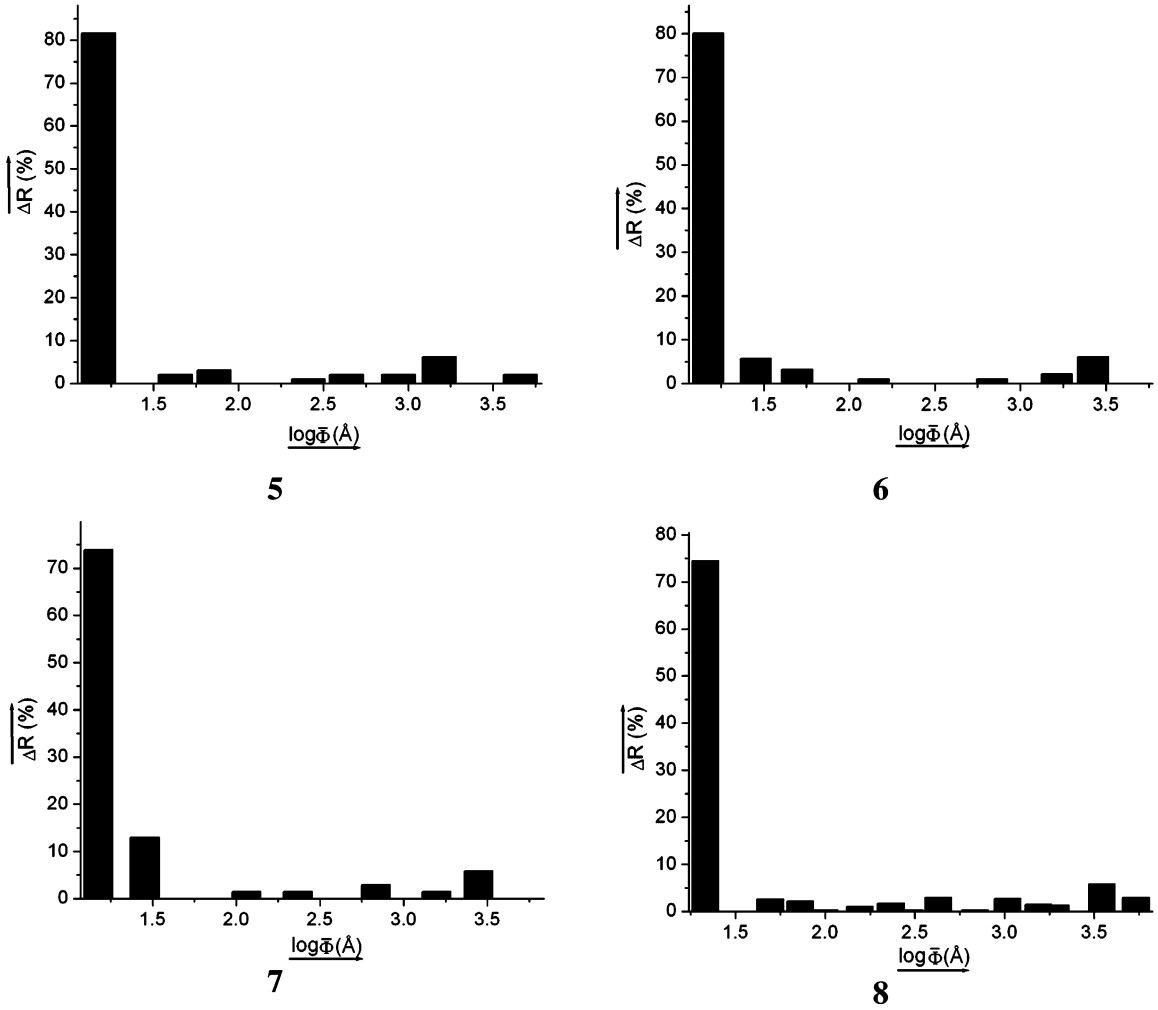

Figure 6. Log $\Phi_{average}$ (Å) vs ΔR (%) for monoliths **5**−**8**.

for 30 min at 0 °C, they were left at room temperature for only 6 h and were then washed with dichloromethane for 30 min at a flow rate of 0.2 mL/min. A solution of 7-oxabicyclo[2.2.1]hept-5-ene-2,3-dicarboxylic anhydride (50 mg, 0.30 mmol) in 1.5 mL of dichloromethane was prepared separately and then pumped into the monolith. The column was heated to 55 °C for 12 h, then cooled to room temperature, and flushed with a solution of 20 vol % ethyl vinyl ether in dimethyl sulfoxide for 8 h at a flow rate of 0.1 mL/min. Finally, all columns prepared were flushed with chloroform for 4 h at a flow rate of 0.2 mL/min. Capacities of functionalized ROMP monoliths were determined by titration versus phenolphthalein using a 0.01 N NaOH solution.

Characterization of Monoliths. Characterization was accomplished applying ISEC according to a published procedure.[43] For the measurements of retention times, 10 μL samples of individual polystyrene standards (0.25 mg/mL) dissolved in the mobile phase (chloroform) were injected into each column, applying a flow rate of 0.6 mL/min. For the determination of the total accessible porosity of the column, a 10 μL sample of benzene was injected. All chromatograms were recorded at a wavelength of 254 nm, at which the response for polystyrene was satisfactory. Retention times and volumes corresponding to each injection were determined from the peak maximum. All retention volumes were corrected for the extra-column volume of the equipment. Calculations were carried out assuming that the hydrodynamic radii of the PS standards in $CHCl_3$ do not differ significantly from those reported in CH_2Cl_2.[43]

9-Oxabicyclo[6.1.0]non-4-ene. At 0−5 °C, a solution of *m*-chloroperbenzoic acid (8.73 g, 97.22 mmol) dissolved in 125 mL of dichloromethane was added dropwise to a solution of 1,5-cyclooctadiene (5.00 g, 92.5 mmol) in 75 mL of dichloromethane. The reaction mixture was allowed to warm to room temperature and was stirred for an additional 4 h. *m*-Chlorobenzoic acid was filtered off, and the filtrate was washed three times with 50 mL of NaOH solution, three times with 50 mL of $NaHCO_3$ solution, and three times with 50 mL of water. Finally, the organic layer was dried over anhydrous Na_2SO_4 and concentrated. Pure product was obtained by distillation at 81−90 °C/14 Torr. Yield: 3.5 g (61%). FT-IR (ATR mode): 3028 (m), 2981 (m), 2852 (m), 2193 (m), 2156 cm^{-1} (m). ^1H NMR ($CDCl_3$): δ 5.64 (m, 2H, 4,5-H), 3.08 (m, 2H, 1,8-H), 2.36−2.5 (m, 2H), 2.0 (m, 2H), 1.89 (m, 4H, 2,3,6,7-H). ^{13}C NMR ($CDCl_3$): δ 129.63, 130.34 (C-4,5), 56.6 (C-1,8), 28.62, 23.72, 22.72 (C-2,3,6,7). GC-MS: t_R = 4.81 min, m/z = 124 (M^+).

4-Cycloocten-1-ol. 9-Oxabicyclo[6.1.0]non-4-ene (1.0 g, 8.1 mmol) was added at room temperature to a suspension of $LiAlH_4$ (168 mg, 4.5 mmol) in 25 mL of diethyl ether. The reaction mixture was stirred for 16 h. Afterward, 5 mL of water was slowly added to the reaction mixture, which was then stirred for another 10 min. Finally, anhydrous $MgSO_4$ (5 g) was added and filtered off after 30 min. The filtrate was collected and concentrated under reduced pressure. Pure product was obtained by distillation at 96−98 °C/14 Torr. Yield: 720 mg (70%). FT-IR (ATR mode): 3319 (b), 3013 (m), 2923 (m), 1465, 1450 cm^{-1} (s). ^1H NMR ($CDCl_3$): δ 5.647, 5.57 (m, 2H, 4,5-H), 3.08 (m, 1H, 1-H), 2.3−1.64 (m,12 H, CH_2). ^{13}C NMR ($CDCl_3$): δ 129.4, 130.24 (C-4, 5), 72.83 (C-1) 37.8/36.39 (C-2,8), 25.75, 24.99, 22.87 (C-3,6,7). GC-MS: t_R = 4.84 min, m/z = 126 (M^+).

Tris(cyclooct-4-enyl-1-oxy)methylsilane. Triethylamine (11 mL, 79 mmol, 3.1 equiv) was added to a solution of cyclooct-5-en-1-ol (3.0 g, 23.8 mmol) in 45 mL of dichloromethane at 0 °C. Then trichloromethylsilane (0.924 mL, 7.86 mmol) was added dropwise. The reaction mixture was stirred in an ice bath for 30 min and

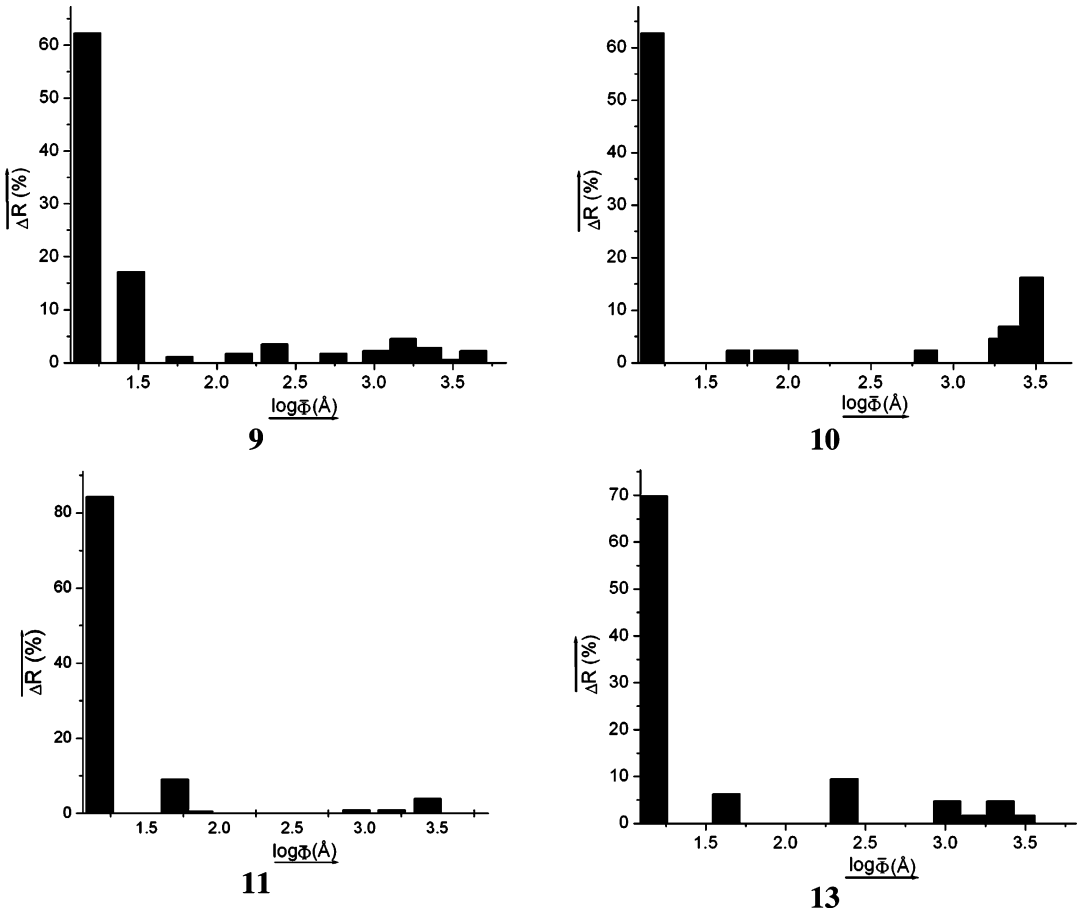

Figure 7. Log $\Phi_{average}$ (Å) vs ΔR (%) for monoliths **9**−**11** and **13**.

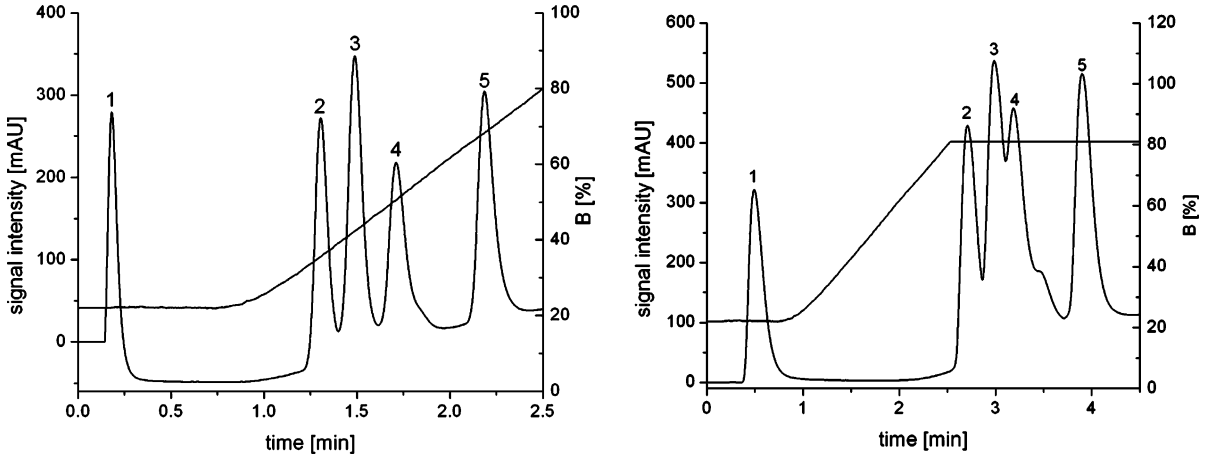

Figure 8. Separation of a protein standard on a COE-derived monolith (left) and NBE-derived monolith (right). Identical column dimensions (3 × 100 mm), mobile phases, and gradients were used (see Experimental Section). Peak order (1) lysozyme A, (2), ribonuclease (3) insulin, (4) cytochrome *c*, (5) myoglobin.

then for a further 2 h at room temperature. The resultant suspension was subsequently washed with 2 × 50 mL portions of water, acetic acid, saturated aqueous sodium bicarbonate, and water. Finally, the dichloromethane layer was dried over anhydrous $MgSO_4$ and concentrated under reduced pressure. Yield: 3.0 g (80%). FT-IR (ATR mode): 3013 (m), 2926, 2854 (m), 1466, 1443 cm^{-1} (s). ^1H NMR ($CDCl_3$): δ 5.58−5.30 (m, 2H, 4,5-H), 4.40 (m, 1H, 1-H), 1.80−2.37 (m, 10 H, CH_2), 0.05 (s, 3H, Si−CH_3). ^{13}C NMR ($CDCl_3$): δ 129.71, 130.24 (C-4,5), 73.01 (C-1) 37.88/36.45 (C-2,8), 25.86, 25.79, 22.79 (C-3,6,7), −5.05 (Si−C). GC-MS: t_R = 14.10 min, m/z = 418 (M^+).

[$RuCl_2(Py)_2(IMesH_2)(CHPh)$].[39] [$RuCl_2(PCy_3)(IMesH_2)(CHPh)$] (100 mg, 0.13 mmol) was dissolved in excess pyridine (0.5 mL), and the mixture was stirred for 5 min. Then pentane was carefully layered over the solution, and the vial was capped and cooled in a freezer overnight. The supernatant was decanted, and the green solid was filtered and washed with 5 × 1 mL portions of pentane. Afterward, it was dried in vacuo at room temperature. Yield: 80 mg (94%). FT-IR (ATR mode): 3058 (m), 2949 (m), 2912 (m), 1601 (m), 1482 (s), 1261 (s), 1071 (m), 850 (m), 756 (m), and 696 cm^{-1} (m). ^1H NMR ($CDCl_3$): δ = 19.16 (Ru=CH), 8.63 (s, 2H), 7.80 (m, 2H), 7.64−7.60 (m, 3H), 7.48 (m, 2H), 7.3−7.28 (m, 2H), 7.07−6.97 (m, 6H), 6.75(m, 2H), 4.07 (m, 4H), 2.64 (s, 6H), 2.35−2.29 (m, 12H). ^{13}C NMR ($CDCl_3$): δ = 218.3, 152.1, 151.3, 150.0, 139.9, 138.2, 137.7, 136.6, 135.8, 134.5, 130.26, 130.1, 129.5, 127.9, 123.8, 123.7, 52.0, 50.8, 21.2, 20.5, 18.5. HRMS calcd for $C_{38}H_{43}RuCl_2N_4$: m/z = 727.191; m/z (found) = 691.22 $(M-Cl)^+$, 612.18 $(M-Cl, -py)^+$, 533.13 $(M-Cl, -2Py)^+$.

Ru Analysis. 30−40 mg samples of the monoliths of interest were dissolved in a minimum amount of aqua regia (typically 5−7 mL) applying microwave irradiation. The digest was transferred to a volumetric flask, and the volume of the solution was adjusted to 10.000 mL. Ru measurements were carried out on an ICP-OES using $\lambda = 267.876$ nm for Ru measurements and $\lambda = 267.840$ and 267.920 nm, for background measurements. The limit of detection (LOD) was 0.02 mg/L. For calibration, Ru-containing aqueous standards (pH = 1, nitric acid) with Ru concentrations of 0, 0.1, 0.5, and 1.0 mg/L were used.

Protein Separation. Monolith recipes: COE:CL:2-PrOH:toluene and NBE:DMN-H6:2-PrOH:toluene = 35:15:40:10 (all wt %), 0.2 wt % initiator, 0.8 mol equiv of pyridine with respect to initiator; column dimensions: 3 × 100 mm (borosilicate columns). Columns were surface functionalized prior to monolith preparation according to published procedures.[25] Mobile phase A: 95% water + 5% acetonitrile + 0.05% TFA; mobile phase B: 20% water + 80% acetonitrile + 0.05% TFA; linear gradient, 22−80% B in 2.5 min, then 80% B up to 4.5 min; flow = 3 mL/min; $T = 25$ °C; UV (200 nm). Analytes: (**1**) lysozyme, (**2**) ribonuclease A, (**3**) insulin, (**4**) cytochrome *c*, and (**5**) myoglobin. Injection volumes were 10 μg for **1**, **2**, **4**, **5** and 13 μg for **3**.

Summary

In summary, we developed entirely novel monolithic matrices based on ring-opened *cis*-cyclooctene and a *cis*-cyclooctene-based cross-linker. These may be tailor-made in terms of porosity, pore size distribution, and specific surface area. In addition, the ROMP-based protocol may again be used for functionalization. The novel rigid rods differ significantly from their norborn-2-ene-based counterparts in that they exhibit significantly higher values for the volume fraction of pores (ϵ_p) and for the specific pore volume (V_p), yet lower values for the volume fraction of the interglobular void volume (ϵ_z). This directly translates into particular separation characteristics, which are different from those of NBE-based materials. Investigations concerning the long-term stability of the novel monoliths as well as applications in micro-HPLC will be reported in due course.

Acknowledgment. Our work was supported by a grant of the Deutsche Forschungsgemeinschaft (DFG, BU2174/1-1) and by the Freistaat Sachsen.

References and Notes

(1) Afeyan, N. B.; Gordon, N. F.; Mazsaroff, I.; Varady, L.; Fulton, S. P.; Yang, Y. B.; Regnier, F. E. *J. Chromatogr.* **1990**, *519*, 1.
(2) Afeyan, N. B.; Fulton, S. P.; Regnier, F. E. *J. Chromatogr.* **1991**, *544*, 267−279.
(3) Rodrigues, A. E. *J. Chromatogr. B* **1997**, *699*, 47−61.
(4) Xu, Y.; Liapis, A. I. *J. Chromatogr. A* **1996**, *724*, 13−25.
(5) Kubin, M.; Spacek, P.; Chromecek, R. *Collect. Czech. Chem. Commun.* **1967**, *32*, 3881−3887.
(6) Hansen, L. C.; Sievers, R. E. *J. Chromatogr.* **1974**, *99*, 123−133.
(7) Hosoya, K.; Ohta, H.; Yoshizoka, K.; Kimatas, K.; Ikegami, T.; Tanaka, N. *J. Chromatogr. A* **1999**, *853*, 11−20.
(8) Maruska, A.; Ericson, C.; Végvári, A.; Hjertén, S. *J. Chromatogr. A* **1999**, *837*, 25−33.
(9) Gusev, I.; Huang, X.; Horváth, C. *J. Chromatogr. A* **1999**, *855*, 273−290.
(10) Tang, Q.; Xin, B.; Lee, M. L. *J. Chromatogr. A* **1999**, *837*, 35−50.
(11) Stachowiak, T. B.; Svec, F.; Frechet, J. M. J. *J. Chromatogr. A* **2004**, *1044*, 97−111.
(12) Xie, S.; Svec, F.; Fréchet, J. M. J. *Chem. Mater.* **1998**, *10*, 4072−4078.
(13) Gerstner, J. A.; Hamilton, R.; Cramer, S. M. *J. Chromatogr.* **1992**, *596*, 173−180.
(14) Tanaka, N.; Nagayama, H.; Kobayashi, H.; Ikegami, T.; Hosoya, K.; Ishizuka, N.; Minakuchi, H.; Nakanishi, K.; Cabrera, K.; Lubda, D. *J. High Resol. Chromatogr.* **2000**, *23*, 111−116.
(15) Tanaka, N.; Kobayashi, H.; Ishizuka, N.; Minakuchi, H.; Nakanishi, K.; Hosoya, K.; Ikegami, T. *J. Chromatogr. A* **2002**, *965*, 35−49.
(16) Rabel, F.; Cabrera, K.; Lubda, D. *Int. Lab.* **2001**, *01/02*, 23−25.
(17) Cabrera, K.; Lubda, D.; Eggenweiler, H.-M.; Minakuchi, H.; Nakanishi, K. *J. High Resol. Chromatogr.* **2000**, *23*, 93−99.
(18) Svec, F. *LC-GC Eur.* **2005**, *18*, 17−20.
(19) Svec, F.; Huber, C. G. *Anal. Chem.* **2006**, *78*, 2100−2107.
(20) Tennikova, T. B.; Reusch, J. *J. Chromatogr. A* **2005**, *1065*, 13−17.
(21) Hilder, E. F.; Svec, F.; Frechet, J. M. J. *J. Chromatogr. A* **2004**, *1044*, 3−22.
(22) Svec, F.; Tennikova, T. B.; Deyl, Z. *Monolithic Materials: Preparation, Properties and Application*; Elsevier: Amsterdam, 2003; Vol. 67, pp 1−773.
(23) Sinner, F.; Buchmeiser, M. R. *Macromolecules* **2000**, *33*, 5777−5786.
(24) Sinner, F.; Buchmeiser, M. R. *Angew. Chem.* **2000**, *112*, 1491−1494*; Angew. Chem., Int. Ed.* **2000**, *39*, 1433−1436.
(25) Mayr, B.; Tessadri, R.; Post, E.; Buchmeiser, M. R. *Anal. Chem.* **2001**, *73*, 4071−4078.
(26) Mayr, M.; Mayr, B.; Buchmeiser, M. R. *Angew. Chem.* **2001**, *113*, 3957−3960*; Angew. Chem., Int. Ed.* **2001**, *40*, 3839−3842.
(27) Mayr, B.; Hölzl, G.; Eder, K.; Buchmeiser, M. R.; Huber, C. G. *Anal. Chem.* **2002**, *74*, 6080−6087.
(28) Lubbad, S.; Mayr, B.; Huber, C. G.; Buchmeiser, M. R. *J. Chromatogr. A* **2002**, *959*, 121−129.
(29) Lubbad, S.; Buchmeiser, M. R. *Macromol. Rapid Commun.* **2002**, *23*, 617−621.
(30) Lubbad, S.; Buchmeiser, M. R. *Macromol. Rapid Commun.* **2003**, *24*, 580−584.
(31) Buchmeiser, M. R.; Sinner, F. Method of Producing Monolithic Support Materials (Verfahren zur Herstellung monolithischer Trägermaterialien). 409 095 (A 960/99, 310599), PCT/EP00/04 768, WO 00/73782 A1, EP 1 190244 B1, 071200, 1999.
(32) Buchmeiser, M. R. *Macromol. Rapid Commun.* **2001**, *22*, 1081−1094.
(33) Buchmeiser, M. R. *J. Mol. Catal. A: Chem.* **2002**, *190*, 145−158.
(34) Buchmeiser, M. R. Rigid Polymers Prepared by Ring-Opening Metathesis Polymerization. In *Monolithic Materials: Preparation, Properties and Applications* (*J. Chromatogr. Library*); Elsevier: Amsterdam, 2003; Vol. 67, pp 103−120.
(35) Buchmeiser, M. R.; Lubbad, S.; Mayr, M.; Wurst, K. *Inorg. Chim. Acta* **2003**, *345*, 145−153.
(36) Lubbad, S.; Steiner, S. A.; Fritz, J. S.; Buchmeiser, M. R. *J. Chromatogr. A* **2006**, *1109*, 86−91.
(37) Buchmeiser, M. R. *New J. Chem.* **2004**, *28*, 549−557.
(38) Meier, H.; Mayer, W.; Kolshor, H. *Chem. Ber.* **1987**, *120*, 685−689.
(39) Love, J. A.; Morgan, J. P.; Trnka, T. M.; Grubbs, R. H. *Angew. Chem.* **2002**, *114*, 4207−4209; *Angew. Chem., Int. Ed.* **2002**, *41*, 4035−4037.
(40) Wang, D.; Yang, L.; Decker, U.; Findeisen, M.; Buchmeiser, M. R. *Macromol. Rapid Commun.* **2005**, *26*, 1757−1762.
(41) Choi, T.-L.; Grubbs, R. H. *Angew. Chem.* **2003**, *115*, 1785−1788*; Angew. Chem., Int. Ed.* **2003**, *42*, 1743−1746.
(42) Sanford, M. S.; Love, J. A.; Grubbs, R. H. *J. Am. Chem. Soc.* **2001**, *123*, 6543−6554.
(43) Halász, I.; Martin, K. *Angew. Chem.* **1978**, *90*, 954−961; *Angew. Chem., Int. Ed.* **1978**, *17*, 901−909.
(44) Halász, I.; Martin, K. *Ber. Bunsen-Ges. Phys. Chem.* **1975**, *79*, 731−732.
(45) Szwarc, M. *Makromol. Chem., Rapid Commun.* **1992**, *13*, 141−145.
(46) Matyjaszewski, K. *Macromolecules* **1993**, *26*, 1787−1788.
(47) Penczek, S.; Kubisa, P.; Szymanski, R. *Makromol. Chem., Rapid Commun.* **1991**, *12*, 77−80.
(48) Johnson, A. F.; Mohsin, M. A.; Meszena, Z. G.; Graves-Morris, P. *J. Macromol. Sci., Rev. Macromol. Chem. Phys.* **1999**, *C39*, 527−560.
(49) Szwarc, M. *J. Polym. Sci., Part A: Polym. Chem.* **1998**, *36*, ix−xv.
(50) Webster, O. W. *Science* **1991**, *251*, 887−892.

MA0609883